Physical Analysis of multimodality in atomization processes

M. R. O. Panão*, A. L. N. Moreira
IN+, Center for Innovation, Technology and Policy Research
Instituto Superior Técnico
Av. Rovisco Pais, 1049-001 Lisboa, PORTUGAL

L. Radu
Faculty of Engineering, Catholic University of Portugal
Estrada Octávio Pato, 2635-631 Rio de Mouro, PORTUGAL

Abstract

This paper reports an analysis of the physics of atomization processes using a Bayesian approach based on a Markov chain Monte Carlo (MCMC) algorithm, taking into account eventual multimodality and heterogeneities in drop size distributions. This approach allows the identification of subgroups in multimodal or heterogeneous drop size distributions, overcoming the limitations of presenting its moments alone and hindering the eventual presence of different natures of droplet formation. The method is assessed with measurements performed on spray impaction and is further applied to physically interpret multijet atomization processes.

Introduction

Statistical analysis is an essential tool for the characterization of atomization processes. Typically, fragmentation of the bulk liquid results in a broad and non-Gaussian size distribution, often dependent on the hydrodynamic mechanisms generating droplets. In the cases where more than one of these mechanisms is present, the drop size distribution characterizing the outcome of atomization may be multimodal or heterogeneous. In the context of the present work, it should be noted that multimodal drop size distributions do not refer to any measurement errors, but due to the physical nature of the fragmentation process.

After having characterized the multiple drop sizes resulting from atomization, it is considered desirable to characterize a certain drop size distribution in terms of a representative drop diameter, for example, the arithmetic mean diameter based on number-weighted size distribution (d_{10}) as in most spray characterization experiments, the Sauter mean diameter, an average based on surface-weighted distributions (d_{32}) as in combustion applications, or the De Brouckere mean diameter based on volume-weighted distributions (d_{43}), as in spray cooling applications [1]. The purpose of using a representative drop diameter in the physical analysis of an atomization process is to replace the polydisperse drop size distribution with a monodisperse one, where each drop diameter is considered to have the same representative size. This latter is further used to analyze the effects of certain operating and environmental conditions upon spray formation. However, although this is a common approach in the characterization of atomization processes its use to physically analyze cases where multimodality or heterogeneities are observed in drop size distributions should be questioned and other statistical methods should be sought that provide a better interpretation of the results obtained. An example of this is when multimodality caused by multiple atomization mechanisms yields different characteristics within the same spray, namely, multiple polydispersions with different evaporative and combustion conditions.

Furthermore, some modeling approaches for polydispersed drop sizes in sprays have been proposed where its full nature is captured by its moments which are further transported using an Eulerian formulation. This apparently suggests the ability to reconstruct, for example, the number-distribution of drop sizes at any point in space and time in the modeling scheme [2, 3]. Therefore, it would be useful to have a method which would provide enough information enabling such reconstruction, as well as to retrieve physical information about the spray.

The main objective of the work presented here is to explore the applicability of using finite mixtures of probability density function in the physical analysis of drop size distributions, since these can better capture some specific or hidden properties of droplets size data such as multimodality and unobserved heterogeneities, using a Bayesian approach based on a Markov chain Monte Carlo (MCMC) algorithm. The assessment of the MCMC approach for the physical interpretation of atomization phenomena is made with data on spray impact experiments where size distributions may be multimodal due to simultaneous presence of primary and secondary droplets close to the impinging surface, which are usually distinguished by the direction of the velocity component normal to

*Corresponding author: mpanao@dem.ist.utl.pt

the impact surface [4]. In the case where spray impact occurs onto a heated surface, multimodality may be due to differences in the mechanisms which produce secondary droplets, either induced by the hydrodynamic mechanisms of drop impact (rebound and splash), multiple interactions of droplets impinging in the vicinity of each other (see [6] for a comprehensive review), or even droplets formed by thermal induced phenomena, such as nucleate boiling [7].

We also wish to address the important issue of whether the model is overfitting the number of components by assessing the point process representations of the posterior densities and see if these figures indicate that mixtures with $K \neq K_{ideal}$ components are overfitting. Finally, after exploring the link between the statistical method and physical interpretation of atomization processes, this will be applied to provide further insight into multijet atomization.

Statistical method

Finite mixture distributions appear in a natural way when the mean of a variable "looks" different among observed subjects. This informal indicator of heterogeneity suggests the use of statistical models involving discrete latent variables such as clustering or latent class models. Finite mixture distributions arise as marginal distributions of such models. These statistical models can also capture many specific properties of real data such as multimodality, skewness, kurtosis and unobserved heterogeneity.

Suppose that a data set $\mathbf{y} = (y_1, \ldots, y_N)$ is available, which consists of N i.i.d. observations of a random variable distributed according to a mixture of fixed K normal distributions:

$$f_{mix}(y_i) = \sum_{k=1}^{K} \eta_k f_N\left(y_i|\mu_k, \sigma_k^2\right) \tag{1}$$

In this setting, we are concerned with the estimation of the component parameters $\boldsymbol{\mu} = (\mu_1, \ldots, \mu_K)$, $\boldsymbol{\sigma^2} = (\sigma_1^2, \ldots, \sigma_K^2)$ and the weight distribution $\boldsymbol{\eta} = (\eta_1, \ldots, \eta_K)$ of the underlying mixture distribution, based on the data $\mathbf{y}$.

For this purpose, we employ two independent but similar approaches: a classical maximum likelihood (ML) estimation based on the expectation-maximization (EM) algorithm and a Bayesian approach based on a Markov chain Monte Carlo (MCMC) algorithm as described in [9].

Each approach is generated by a two-step iterative procedure based on the complete-data likelihood function $p\left(\mathbf{y}, \mathbf{S}|\boldsymbol{\mu}, \boldsymbol{\sigma^2}, \boldsymbol{\eta}\right)$ given by

$$\log p\left(\mathbf{y}, \mathbf{S}|\boldsymbol{\mu}, \boldsymbol{\sigma^2}, \boldsymbol{\eta}\right) = \sum_{i=1}^{N}\sum_{k=1}^{K} \delta_{ik} \log\left(\eta_k f_N\left(y_i|\mu_k, \sigma_k^2\right)\right), \tag{2}$$

where the allocations $\mathbf{S} = (S_1, \ldots, S_N)$ of data points are regarded as the missing data and δ_{ik} is a $0/1$ coding of the allocations S_i: $\delta_{ik} = 1$, if and only if $S_i = k$ (i.e. if the observable y_i comes from component k of the mixture).

The main difference of the Bayesian approach, from the ML approach, is the inclusion of a proper prior distribution on the component parameter, which has a smoothing effect on the mixture likelihood function and reduces the risk of obtaining spurious modes in cases where the EM algorithm leads to degenerate solutions. Nevertheless, both approaches are of interest and they show similar results when applied to our data.

Maximum likelihood

In the ML approach, an estimator for a finite mixture model is found as a maximizer with respect to $\left(\boldsymbol{\mu}, \boldsymbol{\sigma^2}, \boldsymbol{\eta}\right)$ of the logarithm of the complete-data likelihood function (2), which means the ML estimation is based on the EM algorithm.

The EM algorithm is an iterative algorithm with two steps: an expectation step (**E-step**) and a maximization step (**M-step**).

Starting with some initial value for the parameters $\left(\boldsymbol{\mu^{in}}, \boldsymbol{\sigma^{2^{in}}}, \boldsymbol{\eta^{in}}\right)$, the **E-step** consists in conditionally (by data) averaging out the unobserved allocations from the complete-data likelihood function. By doing that, an

updated version of the logarithm of the likelihood function is obtained

$$Q\left(\boldsymbol{\mu},\boldsymbol{\sigma^2},\boldsymbol{\eta}\right)=\sum_{i=1}^{N}\sum_{k=1}^{K}\widehat{\delta}_{ik}\log\left(\eta_k f_N\left(y_i|\mu_k,\sigma_k^2\right)\right),\quad \widehat{\delta}_{ik}=\frac{\eta_k^{in} f_N\left(y_i|\mu_k^{in},\sigma_k^{2\,in}\right)}{\sum_{j=1}^{K}\eta_j^{in} f_N\left(y_i|\mu_j^{in},\sigma_j^{2\,in}\right)}. \tag{3}$$

Subsequently, the **M-step** finds a maximizer $\left(\boldsymbol{\mu^{out}},\boldsymbol{\sigma^{2\,out}},\boldsymbol{\eta^{out}}\right)$ of $Q\left(\boldsymbol{\mu},\boldsymbol{\sigma^2},\boldsymbol{\eta}\right)$, that will be used as the new input value for the parameters. In our case:

$$\begin{aligned}
\eta_k^{out}&=\frac{n_k}{N},\quad n_k=\sum_{i=1}^{N}\widehat{\delta}_{ik},\\
\mu_k^{out}&=\frac{1}{n_k}\sum_{i=1}^{N}\widehat{\delta}_{ik}y_i,\\
\sigma_k^{2\,out}&=\frac{1}{n_k}\sum_{i=1}^{N}\widehat{\delta}_{ik}\left(y_i-\mu_k^{out}\right)^2.
\end{aligned} \tag{4}$$

The entire procedure is repeated until model parameters converge.

One difficulty with the ML approach is that the mixture likelihood function is unbounded, when the variance of some component of the mixture is going to zero, and thus no global maximizer does exists. Another drawback is that sometimes the mixture likelihood function has too many local maximizers that can attract our iteration process. This is mainly the case when some component of the mixture has a small variation, for example if the mixture is overfitting (i.e. when trying to fit a model with too many components). Nevertheless, a local maximizer would always be a consistent and efficient estimator.

One can impose some constrains on the variances of the components and the EM algorithm will avoid all these problems and give a strongly consistent estimator, but the Bayesian approach does just that by choosing a proper prior based partially on this information and by doing so, generating a much more regular posterior distribution.

Markov-chain Monte Carlo

The Bayesian approach to a mixture model, estimates the augmented parameter $\left(\mathbf{S},\boldsymbol{\mu},\boldsymbol{\sigma^2},\boldsymbol{\eta}\right)$ by sampling from the complete-data posterior distribution $p\left(\mathbf{S},\boldsymbol{\mu},\boldsymbol{\sigma^2},\boldsymbol{\eta}|\mathbf{y}\right)$. This posterior is given by Bayes' theorem where

$$p\left(\mathbf{S},\boldsymbol{\mu},\boldsymbol{\sigma^2},\boldsymbol{\eta}|\mathbf{y}\right)\propto p\left(\mathbf{y}|\mathbf{S},\boldsymbol{\mu},\boldsymbol{\sigma^2},\boldsymbol{\eta}\right)p\left(\mathbf{S}|\boldsymbol{\mu},\boldsymbol{\sigma^2},\boldsymbol{\eta}\right)p\left(\boldsymbol{\mu},\boldsymbol{\sigma^2},\boldsymbol{\eta}\right), \tag{5}$$

thus the complete-data posterior is proportional to the complete-data likelihood $p\left(\mathbf{y}|\mathbf{S},\boldsymbol{\mu},\boldsymbol{\sigma^2},\boldsymbol{\eta}\right)$ defined in (2) times the prior $p\left(\boldsymbol{\mu},\boldsymbol{\sigma^2},\boldsymbol{\eta}\right)$ on $\left(\boldsymbol{\mu},\boldsymbol{\sigma^2},\boldsymbol{\eta}\right)$.

The MCMC sampling scheme, is carried out by a two-step iterative procedure known as Gibbs sampling, which is well-adapted to sample from the posterior distribution (5). This procedure can be seen as the Bayesian counterpart of the EM algorithm, here alternately $\left(\boldsymbol{\mu},\boldsymbol{\sigma^2},\boldsymbol{\eta}\right)$ is sampled conditional on knowing $\mathbf{S}$, and $\mathbf{S}$ is sampled conditional on knowing $\left(\boldsymbol{\mu},\boldsymbol{\sigma^2},\boldsymbol{\eta}\right)$.

More precisely, following [9] the Gibbs sampling procedure consists in the following:

1. Parameter simulation conditional on the allocations $\mathbf{S}$:
   (a) Sample $\boldsymbol{\eta}$ from the conditional Dirichlet distribution $p\left(\boldsymbol{\eta}|\mathbf{S}\right)\sim\mathcal{D}\left(e_1\left(\mathbf{S}\right),\ldots,e_K\left(\mathbf{S}\right)\right)$;
   (b) Sample σ_k^2 in each group k from an Inverted Gamma distribution $p\left(\sigma_k^2|\mathbf{S},\mathbf{y}\right)\sim\mathcal{G}^{-1}\left(c_k\left(\mathbf{S}\right),C_k\left(\mathbf{S}\right)\right)$;
   (c) Sample μ_k in each group k from a Normal distribution $p\left(\mu_k|\sigma_k^2,\mathbf{S},\mathbf{y}\right)\sim\mathcal{N}\left(b_k\left(\mathbf{S}\right),B_k\left(\mathbf{S}\right)\right)$;
2. Assign a new allocation for each observation y_i conditional on knowing $\left(\boldsymbol{\mu},\boldsymbol{\sigma^2},\boldsymbol{\eta}\right)$, from the distribution $k\mapsto p\left(S_i=k|\boldsymbol{\mu},\boldsymbol{\sigma^2},\boldsymbol{\eta},\mathbf{y}\right)\propto\eta_k f_N\left(y_i|\mu_k,\sigma_k^2\right)$.

The precise form of $b_k(\mathbf{S})$, $B_k(\mathbf{S})$, $c_k(\mathbf{S})$ and $C_k(\mathbf{S})$ depends upon the chosen prior distribution family, for example if we consider a conditionally conjugate prior:

- $N_k(\mathbf{S}) = \#\{i\colon S_i = k\}$,
- $\overline{y}_k(\mathbf{S}) = \dfrac{1}{N_k(\mathbf{S})} \sum_{i\colon S_i=k} y_i$,
- $s^2_{\mathbf{y},k}(\mathbf{S}) = \dfrac{1}{N_k(\mathbf{S})} \sum_{i\colon S_i=k} \left(y_i - \overline{y}_k(\mathbf{S})\right)^2$,
- $e_k(\mathbf{S}) = e_0 + N_k(\mathbf{S})$,
- $c_k(\mathbf{S}) = c_0 + \dfrac{1}{2} N_k(\mathbf{S})$,
- $C_k(\mathbf{S}) = c_0 + \dfrac{1}{2}\left(N_k(\mathbf{S}) s^2_{\mathbf{y},k}(\mathbf{S}) + \dfrac{N_k(\mathbf{S}) N_0}{N_k(\mathbf{S}) + N_0} \left(\overline{y}_k(\mathbf{S}) - b_0\right)^2\right)$,
- $B_k(\mathbf{S}) = \dfrac{1}{N_k(\mathbf{S}) + N_0} \sigma^2_k$,
- $b_k(\mathbf{S}) = \dfrac{N_0}{N_k(\mathbf{S}) + N_0} b_0 + \dfrac{N_k(\mathbf{S})}{N_k(\mathbf{S}) + N_0} \overline{y}_k(\mathbf{S})$.

The hyperparameters $(e_0, b_0, N_0, c_0, C_0)$ are carefully selected as they may exercise considerable influence on the posterior distribution. For example, one may use the following data-dependent hyperparameters: $e_0 = 4$, $b_0 = \overline{y}$, $N_0 = 2.6/\left(y_{max} - y_{min}\right)$, $c_0 = 2.5$, $C_0 = 0.5 s^2_{\mathbf{y}}$.

Potential Overfitting

At first we attempt to fit finite mixture models with $K \in \{2, 3, 4, 5, 6, 7\}$ normal components. After that, we try to find the ideal value for K informally exploring the sampling representations of the mixture posterior density and the figure that compare the posterior distribution of moments of the marginal distribution for the different models. At the same time, we try to understand from these figures which mixtures are overfitting.

From Figure 1 we try to find above which K the number of clusters begins stabilizing, despite the increase of spreading observed in these simulation clusters. Therefore the point process representation of the MCMC draws will cluster around the point process representation of the true model even if the mixture is overfitting. The draws in Figure 1 point toward the mixture with $K = 4$ as being the ideal mixture and that mixtures with $K = 5$, $K = 6$ and $K = 7$ are possibly overfitting.

To support this argument we look also at Figure 2, where the posterior distribution of moments of the marginal distribution for the different models are compared. Figure 2 indicates that four components are sufficient to capture the moments under investigation, because adding a fifth or a sixth component hardly changes the posterior distribution of these moments. At the same time, we see that two and three components do not seem sufficient because the model unable to reasonably capture the fourth moment (kurtosis). The data in Table 1 also sustains the same conjecture, *i.e.* that the model with the largest marginal likelihood is a mixture of four normal distributions. Therefore, such parameter could be used as a criterion for choosing the most likely mixture.

Table 1. Log of the bridge sampling estimator of the marginal likelihood $p(\mathbf{y}|M_K)$

K	2	3	4	5	6	7
$p(\mathbf{y}\|M_K)$	-48 539	-48 467	-48 363	-48 376	-48 386	-48 393

Assessment of MCMC interpretative value with spray impact experiments

In spray impact flow characterization, droplets impinging on the wall are usually distinguished for those produced by hydrodynamic impact mechanisms through their axial velocity component (u_d), *i.e.* the one perpendicular to the plane of the impact surface. If u_d is positive, droplets are designated as primary, if negative, droplets are secondary and their ensemble corresponds to a secondary spray. The total sample in each measurement point

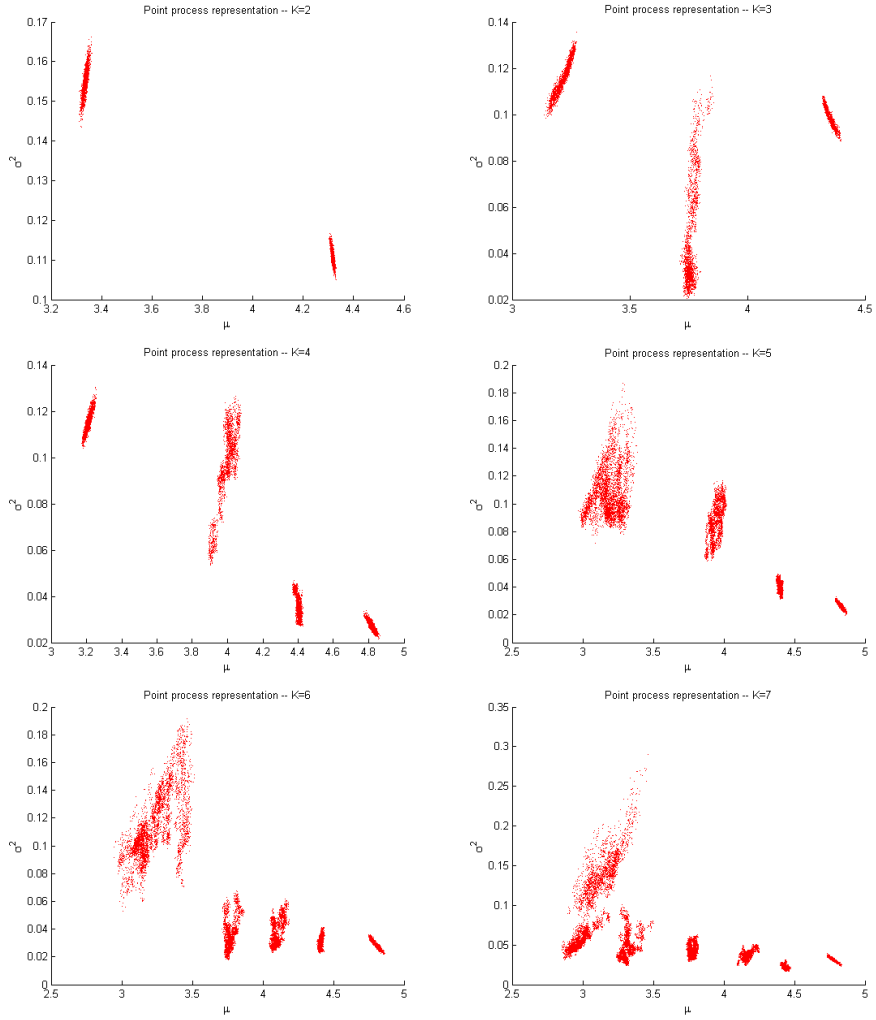

Figure 1. Drop Size Data, normal mixture with $K = 2$ (left-hand side) and $K = 3$ (right-hand side) components; μ plotted against σ^2 for the MCMC draws

includes both kinds. Therefore, experiments on spray impaction are a good starting point to assess the applicability of the MCMC method, since the discrete probability distribution of drop sizes without sorting primary from secondary through the axial velocity component should contain the corresponding sprays.

The experimental data used is reported in Panão and Moreira [4, 5], consisting of a spray impinging onto a 32 mm diameter disc, located 30 mm from the injector and measurements have been made of drop size and 2D-velocity at 2 mm above the wall and radial points depart from the central axis at $r \in \{0, 0.5, 1, 2, 3, 4, 5, 6, 8, 10\}$ mm. Considering the total sample size at each r, the simultaneous presence of primary and secondary droplets implies, at least, that $K = 2$ in the MCMC method. An example of the results obtained is depicted in Figure 3 for $r = 1$ mm.

Primary droplets are usually the larger ones, therefore, $f_N(y|\mu_2, \sigma_2^2)$ in the figure should correspond to these drops, while $f_N(y|\mu_1, \sigma_1^2)$ to secondary droplets. However, the assessment of the approach relies on the accuracy with which $f_N(y|\mu_1, \sigma_1^2)$ actually models the secondary spray. The criterion of the axial velocity is used and the resulting discrete drop size distributions are again curve fitted by a single Normal distribution function of logarithmic drop sizes, except in the case of a clear presence of heterogeneities. This is evidenced in the left plot of Figure 4, corresponding to primary droplets, where a bimodal appearence implies the application of MCMC at least with $K = 2$ in order to tak einto account the cluster of smaller droplets.

The underlying reason for this cluster is the re-entrainment and eventual re-impact of secondary droplets dragged by vortical flow structures induced by the interaction between the impinging spray and the surrounding air, as reported by Hardalupas [10] and Panão and Moreira [4, 5]. It is reasonable to think that the mean, μ_1,

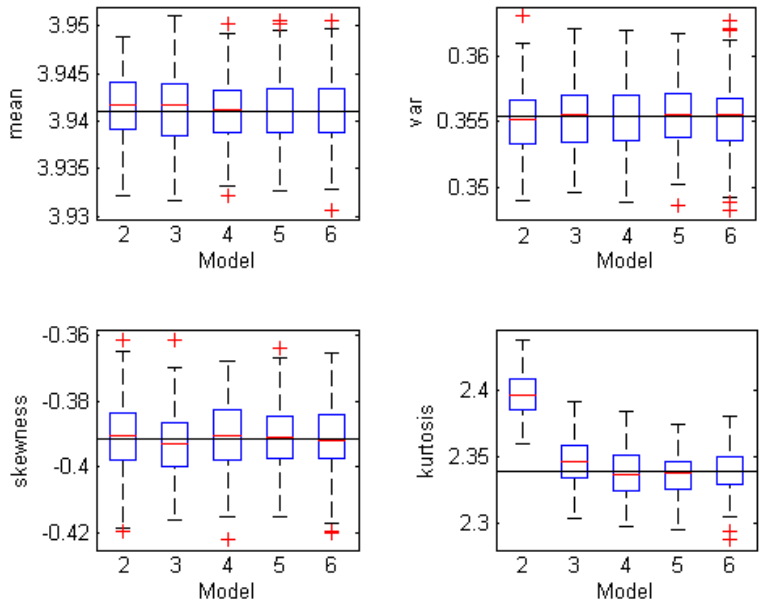

Figure 2. Drop Size Data, posterior distribution of moments; $K \in \{2, 3, 4, 5, 6\}$

obtained for the total sample size (Figure 3), and associated with re-entrained secondary droplets, differs from the mean of droplets with a negative axial velocity $(u_d < 0)$, μ_S, being the former a summation of the parcels of the latter and μ_{P1} (Figure 4-left).

To verify this, one can demonstrate that $\mu_1 = \mu_{P1} + \eta_S (\mu_S + \mu_{P1})$, where η_S is the probability of finding a secondary droplet with a negative axial velocity among the total sample size of measured droplets. An overall value for this coefficient can be easily obtained by dividing the number those secondary droplets (N_S) by the total sample size (N_T), $\eta_S = N_S/N_T$. The differences obtained in all measurement points between μ_1 identified by MCMC and the estimation given by the expression above were less than 2.6%.

The spray impingement flow demonstrates how a known statistical tool of mixing probability distribution functions (MCMC) applied to multimodal or heterogeneous drop size distributions is coherent with the physical interpretation, which, in this case, was already known from previous research works. The following is a case-study where we attempt to apply this methodology to physically interpret statistical data and identify the eventual presence of multiple and co-existent hydrodynamic mechanisms in sprays formed by the simultaneous impact of multiple cylindrical jets.

Case-study: multijet atomization

The multijet atomization consists of a liquid disintegration process which generates droplets of polydispersed sizes through the simultaneous impact of N_j cylindrical jets. Most experimental work performed in this atomization strategy is dedicated to the impact of 2 jets, and research works focusing their argument on the impact of more than 2 are scarce. In a previous work [17] it has been observed that more than 2 jets generate a spray from tridimensional structures with periodic patterns associated with the formation of ligaments and further disruption into droplets. The characteristics of these droplets have been measured for several points in a measurement grid using a Phase-Doppler Interferometer which details on the optical configuration can be found in [17].

In this work, the MCMC approach used to physically interpret liquid atomization considers the entire spray, thus, the data used contains all the the information collected within the measurement grid established for each atomizer. Simulations consider mixtures of $K \in \{1, 2, 3, 4, 5[\text{only for } N_j = 2]\}$ and the best fit is not solely based on the marginal likelihood $p\,(y|M_K)$, but also the analysis of the weights η_k, since better marginal likelihoods can be obtained with an additional function, although its weight is relatively low, meaning its presence has only an overall compensating value within the finite mixture distribution. The results for η_k and the marginal likelihood $p\,(y|M_K)$ plotted in the left side of Figure 5 show that:

- for $N_j = 2$ above $K \geq 2$ the marginal likelihood slightly increases, however, in the highest value at

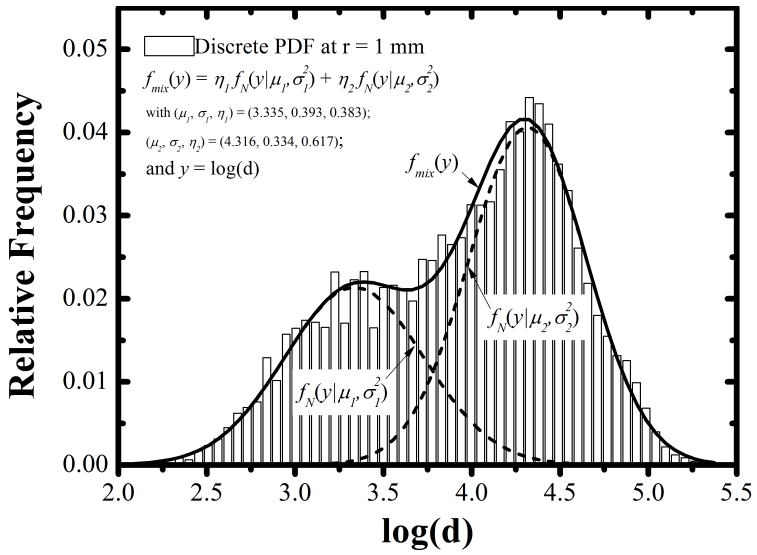

Figure 3. Discrete drop size distribution of a spray impact experiments [4, 5] at $r = 1$ mm and the results obtained by MCMC for $K = 2$ Log-Normal distribution functions.

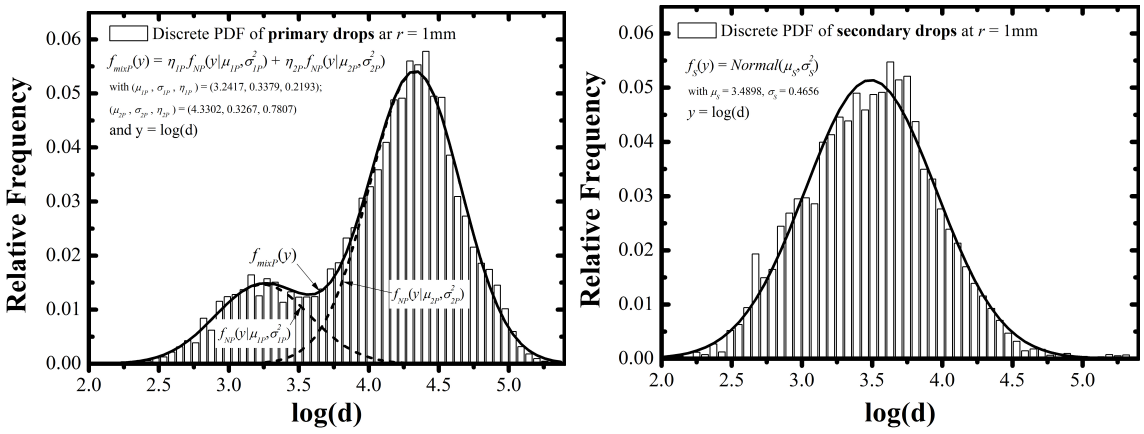

Figure 4. Discrete drop size distribution of a spray impact experiments [4, 5] at $r = 1$ mm and the results obtained by MCMC for $K = 2$ Log-Normal distribution functions.

$K = 5$, $\eta_{k,k\in\{1,4,5\}}$ are (in percentage) 0.1%, 7% and 2%, respectively, therefore, could be considered as compensating functions, with no significant meaning, which overfit the actual result. The case for a mixture of $K = 4$ has a $\eta_1 = 0.0007$ suggesting that $K = 3$ might be a better and simpler solution, but $p(y|M_3) < p(y|M_2)$, which allows to conclude that $K = 2$ is enough to accurately describe drop spectra in the atomizer with $N_j = 2$;

- for $N_j = 3$ at $K \geq 2$, marginal likelihood begins stabilizing, however, also for $K = 4$, η_1 and η_4 represent 0.1% and 5%, respectively, which means that $K = 2$ might be a simpler and still accurate solution. With $K = 3$, $\eta_1 = 0.0012$ also pointing to $K = 2$;

- finally, for $N_j = 4$ a certain cascade effect occur because with $K = 4$, $\eta_1 = 0.004$ suggesting that $K = 3$ might be a better and simpler solution, however, with $K = 3$, η_1 has the same value as when four normal distribution functions are mixed, therefore, it points to a compensating function with no physical meaning. This suggests that $K = 2$ is the simplest and best mixing solution to describe drop size distributions produced by a multijet spray with $N_j = 4$.

The mixture which best describes droplet distribution for the multijet spray in all atomizers, with $K = 2$, indicates that there are two dominant groups of droplets, eventually implying two atomization mechanisms. As depicted on the top-right plot of Figure 5, these groups have distinct sizes, however, while the group of larger droplets $\left(\mu_2, \sigma_2^2\right)$ does not significantly change between atomizers, except for a slight increase in the mean, the group of smaller droplets $\left(\mu_1, \sigma_1^2\right)$ is not affected in the mean, but in the polydispersion associated with the variance, especially for $N_j = 4$.

Moreover, the down-right plot in Figure 5 evidences that both droplet groups have similar weights in the $N_j = 2$ atomizer, but as one increases the number of jets, the first group of smaller droplets is ameliorated, which allows the conclusion that whatever mechanism generates group 2, it is the main one producing the spray and is expected to be the same regardless the number of impinging jets.

The results for $K = 2$ are also depicted in Figure 6 in the form of probability distribution of the logarithmic drop size. Here, the effect of weight reduction of the smaller drops group becomes clearer.

To illustrate the physical interpretation deduced from the statistical method applied to drop size measurements, Figure 7 contains images taken for each multijet spray. The structure of the impinging jets is clearly turbulent and the spray pattern formed by their impact has been identified early by the work of Heidmann *et al.* [18] as a *fully developed* pattern characterized by waves of droplets which appear to project from the point of jet impact and exhibit a pattern of lines of drops regularly spaced and a rippled sheet. Santoro and Anderson [19] describe this regularity with three types of periodic structures (identified in Figure 7): 1) surface waves; 2) edge ligaments; 3) and detached ligaments. The latter can be considered the main atomization mechanism and as been correlated with the geometric parameters for two impinging jets atomization (see [20, 21]) as $d_d = 2.217 \cdot d_j \left(We_j f(\theta)\right)^{-0.354}$, where d_d is the drop diameter, We_j the jet Weber number $\left(We_j = \rho_f U_j^2 d_j / \gamma_f\right)$ and $f(\theta) = (1 - cos\theta)^2 / sin^3\theta$. If we use this correlation on the geometric configuration of our multijet experiments with methanol $\left(d_j = 0.4mm; U_j \simeq 8m/s; \theta = 45°; \rho_f = 791.8kg \cdot m^{-3}; \gamma_f = 0.0224N/m\right)$, the expected average drop size is 4.881 μm, which is close to the overall value of 3.7 μm obtained for the three atomizers (see top-right plot in Figure 5). Following this insight, the physical interpretation of the statistical results depicted in Figure 6 is that, for $N_j = 2$, the formation of droplets through edge ligaments is as likely to occur as those formed through ligament detachment in surfaces waves propagating from the impact point (both have similar weights η_k), however, the inclusion of more jets tends to mitigate such drop size group. Also, the similar characteristics of the group of droplets produced from detached ligaments imply that the same atomization mechanism is probably at work independent of the number of atomizers. Nevertheless, further studies are required to verify this at a more fundamental level.

Concluding remarks

The research question addressed in this paper is whether statistics can improve the physical interpretation of atomization processes when drop size distributions are characterized as multimodal and heterogeneous, limiting the accuracy of using average drop sizes. Therefore, it is suggested that the physical interpretation of drop spectra by finite mixtures of distribution functions improves the understanding of the atomization process and the possible coexistence of multiple mechanisms.

In this work,a Markov chains Monte-Carlo approach is pursuit as the statistical method which enables the characterization of finite mixtures of K probability density functions describing multimodal and heterogeneous drop size distributions. Here, mixture of normal distributions have been considered to accurately describe drop

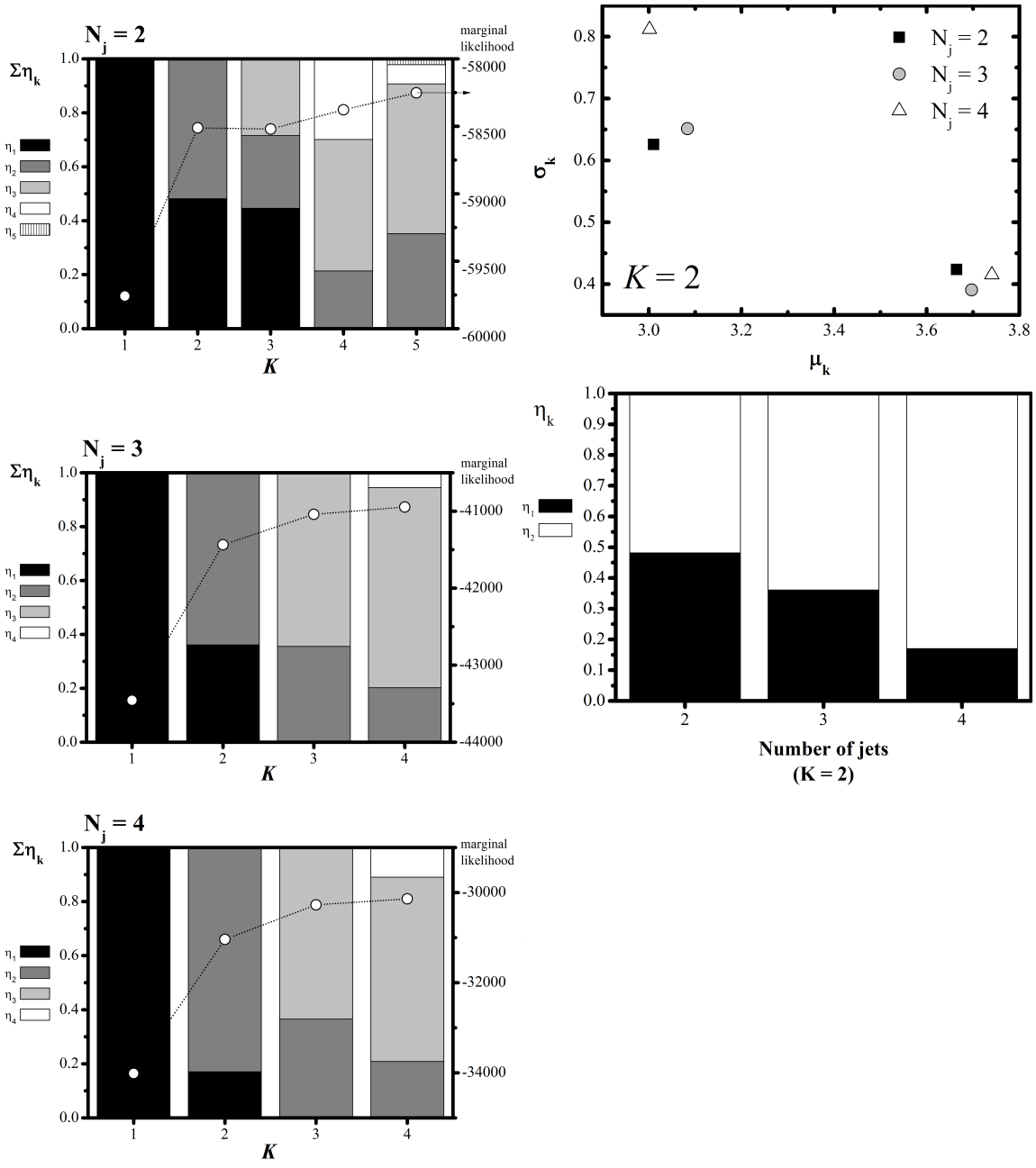

Figure 5. (Left)Weight distribution as function of K and the corresponding Marginal likelihood $p\,(y \mid M_K)$ and (right) Results obtained for the mean μ_k and standard deviation σ_k in a $K = 2$ mixture of Normal distributions for the atomizers with $N_j = 2, 3, 4$.

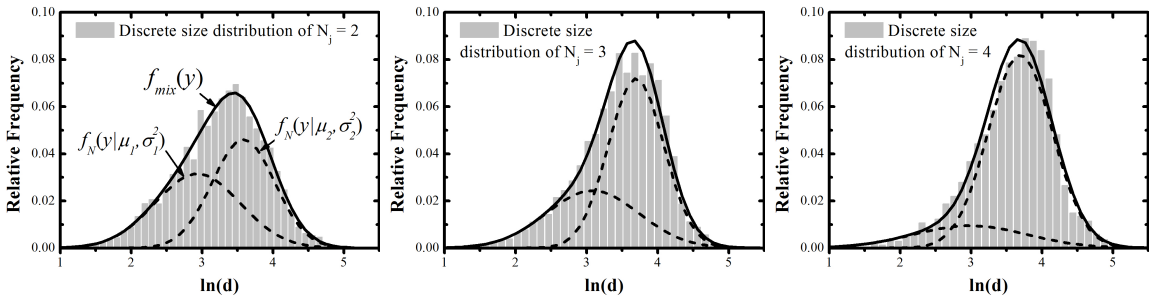

Figure 6. Mixed Normal distribution function with $K = 2$ for the atomizers with $N_j = 2, 3, 4$.

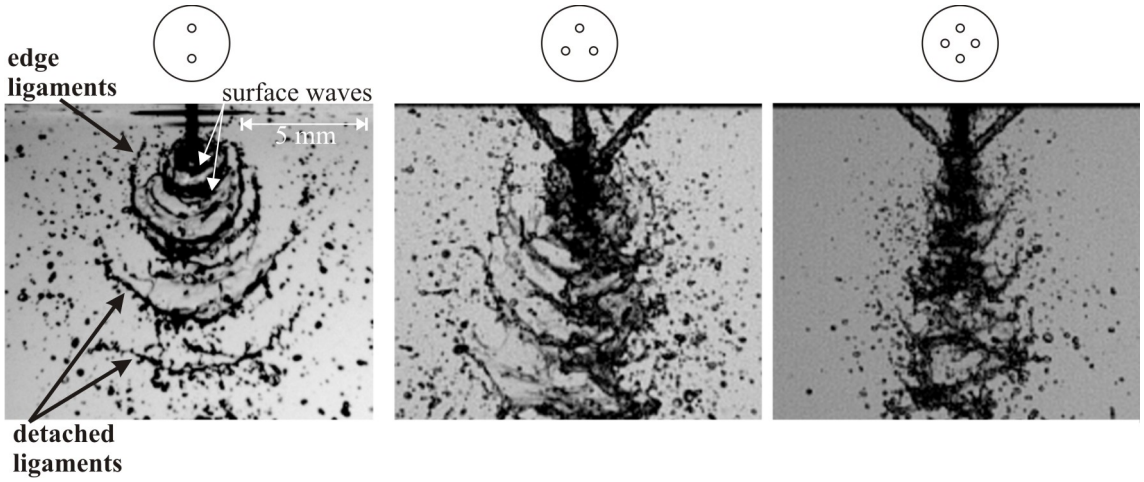

Figure 7. Illustration of the atomization process for $N_j = 2, 3, 4$, including the top-view of jet exit positioning relatively to the side-view of the spray.

size spectra emphasizing the multiplicative nature of the atomization process, although the method is valid for other distribution functions as well.

A description of the statistical method is presented as well as guidelines for a proper interpretation of its results. Then, the approach is assessed by using spray impact experiments where the physical interpretation is known *a priori*. Thereafter, the method is applied to study the characteristics of multiple impinging jets sprays (or multijet sprays), consisting of an atomization strategy which produces droplets from the simultaneous impact of N_j cylindrical jets. The possibility of coexisting multiple atomization mechanisms generating different groups of drop sizes within the multijet spray is investigated. The results not only confirm the presence of two groups of droplets generated from edge and detached ligaments, as in earlier research work developed for $N_j = 2$, but also identifies the latter as the main atomization mechanism, in such way as to dominate over the former when the number of impinging jets N_j increases.

Acknowledgement

The authors would like to acknowledge FCT - Fundação para a Ciência e Tecnologia for the financial support through project PTDC/EME-MFE/099040/2008 and M.R.O Panão would like to acknowledge FCT as well for supporting his research through Grant SFRH/BPD/45170/2008.

Nomenclature

d_{10}	arithmetic mean diameter [μm]
d_{32}	Sauter mean diameter [μm]
d_{43}	De Brouckere mean diameter [μm]
d_d	general drop diameter [μm]
d_j	jet diameter [mm]
f_{mix}	mixture distribution function
f_N	Normal distribution function
K	number of distribution function in mixture
N	number of droplets
N_j	number of impinging jets
$p(y\|M_K)$	marginal likelihood
u	axial droplet velocity [m·s^{-1}]
U_j	jet velocity [m·s^{-1}]
y	logarithm of drop size [μm]

Greek symbols

γ	surface tension [N·m^{-1}]
η	weight of a certain distribution function in the mixture
μ	mean of a Normal distribution

θ impinging jet half-angle [$\circ$]
ρ density [kg·s^{-3}]
σ standard deviation of a Normal distribution

Subscripts

d droplet
f fluid
P primary drop
S secondary drop
T total

Acronyms

MCMC	Markov Chain Monte Carlo
ML	maximum likelihood

References

[1] Sowa, W.A., *Atomization and Sprays* 2:1-15 (1992).
[2] Beck, J.C. and Watkins, A.P., *Proceedings of the Royal Society of London A* 459:1365-1394 (2003).
[3] Archambault, M.R., *Atomization and Sprays* 19:1171-1191 (2009).
[4] Panão, M.R.O. and Moreira, A.L.N., *Experiments in Fluids* 37:834-855 (2004).
[5] Panão, M.R.O. and Moreira, A.L.N., *Experiments in Fluids* 39:364-374 (2005).
[6] Moreira, A.L.N., Moita, A.S. and Panão, M.R.O., *Progress in Energy and Combustion Science* doi:10.1016/j.pecs.2010.01.002 (2010).
[7] Moita, A.S. and Moreira, A.L.N., *Experiments in Fluids* 47:755-768 (2009).
[8] Babinsky, E. and Sojka, P.E., *Progress in Energy and Combustion Science* 28:303-329 (2002).
[9] Frühwirth-Schnatter, S., *Finite Mixture and Markov Switching Models*, NewYork: Springer, 2006.
[10] Hardalupas, Y., Okamoto, S., Taylor, A. M. K. P. and Whitelaw, J. H., *Proceedings of the 6th Int Symp Laser Tech and Appl in Fluid Mech., Lisbon, Portugal* 490-506 (1992).
[11] Roisman, I.V., Horvat, K. and Tropea, C., *Physics of Fluids* 18:102104 (2006).
[12] Yoon, S.S. and Heister, S.D., *Atomization and Sprays* 13:499-516 (2003).
[13] Yoon, S.S. and DesJardin, P.E., *International Journal for Numerical Methods in Fluids* 50:469-489 (2006).
[14] Marmanis, H. and Thoroddsen, S.T., *Physics of Fluids* 8:1344-1346 (1996).
[15] Wang, A.-B., Chen, C.-C. and Hwang, W.-C. in: Rein, M.(ed), *Drop-surface interactions*, Springer, 2002.
[16] Panão, M.R.P and Moreira, A.L.N., *Measurement Science & Technology* 19:095402 (2008).
[17] Panão, M.R.O., Rosa, J.L.C.V., Moreira, A.L.N., 11^{th} *International Conference on Liquid Atomization and Spray Systems*, Colorado, USA, July 2009.
[18] Heidmann, M.F, Priem, R.J., Humphrey, J.C., "A study of sprays formed by two impinging jets", NACA Technical Note 3835, March 1957.
[19] Santoro, R.J., Anderson, W.E., "Combustion instability phenomena of importance to liquid propellant engines", Final Report 1 July 1991 - 30 June 1994.
[20] Dombrowski, N. and Hooper, P.C., *Journal of Fluid Mechanics* 18:392-400 (1964).
[21] Anderson, W.E., Ryan, H.M., Pal, S., Santoro, R.J., "Spray formation processes of impinging jet injectors", Report N94-23042, 1994.